BULLETIN OF THE POLISH ACADEMY OF SCIENCES
TECHNICAL SCIENCES, Vol. 70(3), 2022, Article number: e141307
DOI: 10.24425/bpasts.2022.141307

Robust zeroing neural networks with two novel power-versatile activation functions for solving dynamic Sylvester equation

Peng ZHOU [1] **and Mingtao TAN** [2]*

[1] College of Electronic Information and Automation, Guilin University of Aerospace Technology, Guilin 541004, China
[2] School of Computer and Electrical Engineering, Hunan University of Arts and Science, Changde 415000, China

Abstract. In this work, two robust zeroing neural network (RZNN) models are presented for online fast solving of the dynamic Sylvester equation (DSE), by introducing two novel power-versatile activation functions (PVAF), respectively. Differing from most of the zeroing neural network (ZNN) models activated by recently reported activation functions (AF), both of the presented PVAF-based RZNN models can achieve predefined time convergence in noise and disturbance polluted environment. Compared with the exponential and finite-time convergent ZNN models, the most important improvement of the proposed RZNN models is their fixed-time convergence. Their effectiveness and stability are analyzed in theory and demonstrated through numerical and experimental examples.

Key words: recurrent neural network (RNN); zeroing neural network (ZNN); RZNN; fixed-time convergence.

1. INTRODUCTION

Sylvester equations are frequently encountered in the fields of pure and applied mathematics. Developing efficient algorithms for finding the solutions of Sylvester equations has attracted a lot of interest, due to its wide application in stabilization analysis [1], image processing [2, 3] and disturbance decoupling [4]. In recent years, numerous approaches have been proposed to solve Sylvester equations, such as iterative algorithms [5–10], the matrix sign function method [11], gradient-based neural networks (GNN) [12, 13] and ZNN [14–17].

Note that the iterative algorithms and MSFM are effective for solving the static Sylvester matrix equation. However, computation will increase as the matrix dimension increases, which limits their application in the situation that requires real-time online calculation [18]. GNN is one of the promising approaches to solving static Sylvester matrix equations with high dimension and other linear matrix equations, due to its unique superiority of parallel processing. Since the GNN method does not take time derivative information of the corresponding matrix into consideration, it cannot be directly applied to the dynamic Sylvester matrix equation. Thus, in ref. [19, 20], a ZNN is established to address the dynamic case with fast computation. However, the convergence of ZNN is sensitive to the selection of activation functions (AFs). Specifically, the ZNN model constructed by different AFs will lead to different performance in the process of dynamic problem solving. Inspired by this, many new AFs are reported to improve its exponential convergence performance in [21, 22]. Furthermore, a finite-time convergent ZNN model activated by sign-bi-power AF (SBPAF) is reported in [23].

In practical applications, the ubiquitous noise may greatly decrease the accuracy and efficiency of various time-varying systems. For example, the offset errors in hardware implementation can be considered as the linear-form time-varying disturbances. External signals interference, e.g. electromagnetic interference, can be considered as the superposition of sine-form time-varying disturbances. The instantaneous decline of power sources equipped with the control module can be described as the exponential-decay-form time-varying disturbances. Thus, a number of anti-noise ZNN models have been proposed to address such an issue in the last few years [24–28]. In [29, 30], a NTZNN model is developed to work in the environment of noise and interference. However, all the above mentioned anti-noise ZNN models can only achieve exponential convergence. In ref. [31], a versatile activation function (VAF) is applied to guarantee fixed-time convergence and anti-interference capability of the ZNN model. Although the predefined-time convergence and robustness of the VAF-activated ZNN model [31] can be guaranteed, these superior performances can be further improved. Thus, promotion of the robustness and convergence of the ZNN model is still open.

Motivated by the above discussions, two new RZNN models are proposed by introducing two novel PVAFs in this work to further improve its convergence and robustness simultaneously. It is worth mentioning that the VAF in ref. [31] is just a special case of our new proposed PVAF. Consequently, the main contributions of this work are summarized below.

1. In this work, two RZNN models adopting two novel PVAFs are presented and investigated for online fast solving of the DSE problem in noise-polluted environment.

*e-mail: lightsdu@sina.cn

Manuscript submitted 2022-02-25, revised 2022-04-17, initially accepted for publication 2022-04-24, published in June 2022.

2. Differing from most conventional ZNN models, the proposed RZNN models achieve predefined-time convergence and resist the effect of noises.
3. Rigorous mathematical analysis is presented to prove that the RZNN models can solve the DSE problem within a predefined time.
4. Numerical and experimental examples of the proposed RZNN-based robot trajectory tracking further demonstrate their practical application prospects.

For the convenience of reading, the full names of abbreviations are listed as follows.

Dynamic Sylvester equation	DSE
Zeroing neural network	ZNN
Noise-tolerant ZNN	NTZNN
Power-versatile activation functions	PVAF
Linear activation function	LAF
Power activation function	PAF
Bi-power activation function	BPAF
Power-sigmoid activation function	PSAF
Hyperbolic sine activation function	HSAF
Versatile activation function	VAF
Dynamic bounded disappearing noise	DBDN
Dynamic bounded non-disappearing noise	DBNDN
Mobile robotic manipulator	MRM

2. PROBLEM FORMULATION

As a basis for discussion, the problem formula of DSE is put forward first. Afterwards, the construction procedure of the ZNN model is introduced in detail.

2.1. DSE problem

The following famous Sylvester equation is considered in this paper.

$$D(t)X(t)-X(t)G(t)=-M(t)\in\mathbb{R}^{n\times n}, \tag{1}$$

where t is time, $D(t)$, $G(t)$ and $M(t)$ are known dynamic matrices, and $X(t)\in\mathbb{R}^{n\times n}$ is the unknown time-varying matrix that needs to be calculated. Here, we suppose that there exists a unique solution for the DSE in (1). Then, we can rewrite the DSE in vector form, as follows.

$$\left(I^T\otimes D-G^T\otimes I\right)\mathrm{vec}(X)=-\mathrm{vec}(M), \tag{2}$$

where I is an appropriate size identity matrix, the symbol $\otimes$ represents Kronecker product and $\mathrm{vec}(\cdot)$ represents matrix vectorization. The dynamic matrices $D(t)$, $G(t)$ and $M(t)$ can be selected arbitrarily as long as the coefficient matrix $\left(I^T\otimes D-G^T\otimes I\right)$ is invertible such that DSE (1) has a unique solution.

Define $X^*(t)$ as the unique dynamic solution of DSE (1), the main objective is to design two RZNN models, such that the time-independent neural state solution $X(t)=X^*(t)$ can be obtained in fixed-time even under the condition of noises and interference.

2.2. ZNN for solving DSE

Implementation of the ZNN model for solving DSE (1) described as below [19, 20].

Firstly, dynamic error matrix $E(t)$ is defined.

$$E(t)=D(t)X(t)-X(t)G(t)+M(t)\in\mathbb{R}^{n\times n}. \tag{3}$$

It can be found that the theoretical solution of DSE (1) can be obtained as long as each element of $E(t)$ converges to zero. Then, to force each element of $E(t)$ to converge to 0, we design the following evolution formula:

$$\frac{\mathrm{d}E(t)}{\mathrm{d}t}=-\lambda\Gamma(E(t)), \tag{4}$$

where $\Gamma(\cdot)$: $\mathbb{R}^{n\times n}\to\mathbb{R}^{n\times n}$ is an AF array and $\lambda>0$ is a design parameter.

Finally, substituting equation (3) into (4) yields:

$$\begin{aligned}D(t)\dot{X}(t)-\dot{X}(t)G(t)=&-\dot{D}(t)X(t)+X(t)\dot{G}(t)-\dot{M}(t)\\&-\lambda\Gamma\left(D(t)X(t)-X(t)G(t)+M(t)\right).\end{aligned} \tag{5}$$

Note that the ZNN model in (5) is stable as long as the AF $\Gamma(\cdot)$ is a monotonically increasing odd function [19].

Since AF is an important part of the ZNN model, much effort has been made to develop different AFs to further optimize its convergent performance. These AFs are summarized in Table 1.

Table 1
Existing AFs

Activation functions	Formulations
LAF	$\tau(x)=x$
PAF	$\tau(x)=x^k \quad k>3$ and k is an odd integer
BPAF	$\tau(x)=\left(1-\exp(-\varsigma x)\right)\left(1+\exp(-\varsigma x)\right)$
PSAF	$\tau(x)=\begin{cases}x^p, & \lvert x\rvert\geq 1\\ \dfrac{1+e^{-\xi}-e^{-\xi x}}{1-e^{-\xi}+e^{-\xi x}}, & \text{otherwise}\end{cases}$
HSAF	$\tau(x)=\dfrac{(\exp(\varsigma x)-\exp(-\varsigma x))}{2}, \quad \varsigma>1$
SBPAF	$\tau(x)=\dfrac{\left(\lvert x\rvert^k+\lvert x\rvert^{1/k}\right)\mathrm{sgn}(x)}{2}, \quad 0<k<1$
VAF	$\tau(x)=(a_1\lvert x\rvert^{\eta}+a_2\lvert x\rvert^{\omega})\,\mathrm{sgn}(x)+a_3x+a_4\mathrm{sgn}(x)$

In an ideal no-noise environment, all the AFs in Table 1 can ensure the convergence and stability of the ZNN. Additionally, the ZNN activated by SBPAF achieves finite-time convergence. Moreover, the VAF-based ZNN in ref. [31] achieves both fixed-time convergence and noise resistance. Although the fixed-time convergence and robustness of the VAF-based ZNN model can be guaranteed simultaneously, these superior performances can be further improved, and two new RZNN models adopting two novel PVAFs are proposed in this work exactly to this end.

3. ROBUST ZEROING NEURAL NETWORK (RZNN) MODELS

As mentioned above, robustness of the ZNN models activated by the AFs in Table 1 to noise is not satisfactory. However, noises are inevitable for dynamic systems, and many time-varying systems are sensitive to interference and noise. Therefore, the following two novel PVAFs are proposed to activate the ZNN model, such that both noise resistance and predetermined time convergence can be guaranteed.

$$\tau_1(x) = (a|x|^p + b|x|^q)^k \operatorname{sgn}(x) + c_1 x + c_2 \operatorname{sgn}(x), \tag{6}$$

$$\tau_2(x) = (a|x|^p + b)^k \operatorname{sgn}(x) + d_1 x + d_2 \operatorname{sgn}(x), \tag{7}$$

where $a,\ b,\ p,\ q,\ k > 0$, $pk > 1$, $qk < 1$. To avoid confusion, the AFs in (6) and (7) are defined as PVAF-1 and PVAF-2, respectively.

From equation (6), it can be observed that the VAF in Table 1 is a special case of the PVAF-1 with $k = 1$.

Employing the PVAF-1 and PVAF-2 to $\Gamma(\cdot)$ in equation (5) yields the following two models, respectively, which are expressed as the RZNN-1 model and RZNN-2 model.

$$\begin{aligned} D(t)\dot{X}(t) - \dot{X}(t)G(t) = &-\dot{D}(t)X(t) + X(t)\dot{G}(t) - \dot{M}(t) \\ &- \lambda\Gamma_1(D(t)X(t) - X(t)G(t) + M(t)), \end{aligned} \tag{8}$$

$$\begin{aligned} D(t)\dot{X}(t) - \dot{X}(t)G(t) = &-\dot{D}(t)X(t) + X(t)\dot{G}(t) - \dot{M}(t) \\ &- \lambda\Gamma_2(D(t)X(t) - X(t)G(t) + M(t)). \end{aligned} \tag{9}$$

Taking additive noises into consideration, the RZNN-1 and RZNN-2 models can be presented below.

$$\begin{aligned} D(t)\dot{X}(t) - \dot{X}(t)G(t) = &-\dot{D}(t)X(t) + X(t)\dot{G}(t) - \dot{M}(t) \\ &- \lambda\Gamma_1(D(t)X(t) - X(t)G(t) + M(t)) + N(t), \end{aligned} \tag{10}$$

$$\begin{aligned} D(t)\dot{X}(t) - \dot{X}(t)G(t) = &-\dot{D}(t)X(t) + X(t)\dot{G}(t) - \dot{M}(t) \\ &- \lambda\Gamma_2(D(t)X(t) - X(t)G(t) + M(t)) + N(t), \end{aligned} \tag{11}$$

where $N(t)$ is the matrix noise.

Their robustness and fixed-time convergence will be analyzed in the following section.

4. RZNN MODELS ANALYSIS

To analyze the convergence of the RZNN models, two Lemmas are imposed below.

Lemma 1. [32–34] considering the following dynamic system:

$$\dot{x}(t) \le -\left(ax^p(t) + bx^q(t)\right)^k, \tag{12}$$

where $a,\ b,\ p,\ q,\ k > 0$, $pk > 1$, $qk < 1$. The above dynamic system is predefined-time stable, and $x(t)$ converges to 0 within $T_{\max}$, which is given as:

$$T_{\max} \le \frac{1}{a^k(pk-1)} + \frac{1}{b^k(1-qk)}. \tag{13}$$

Lemma 2. [32–34] considering a dynamic system of the following form:

$$\dot{x}(t) \le -\left(ax^p(t) + b\right)^k, \tag{14}$$

where $a,\ b,\ p,\ q,\ k > 0$, $pk > 1$, $qk < 1$. The above dynamic system is also predefined-time stable, and $x(t)$ converges to 0 within $T_{\max}$.

$$T_{\max} \le \frac{1}{b^k}\left(\frac{b}{a}\right)^{1/p}\left(1 + \frac{1}{pk-1}\right). \tag{15}$$

It is worth noting that the convergent time $T_{\max}$ is independent of the initial state $x(t=0)$, and it can be computed directly with the dynamic parameters a, b, p, q and k.

4.1. RZNN-1 model analysis

Based on Lemma 1, we will firstly analyze the solution of DSE (1) by using the RZNN-1 model in the cases without noise and with various noises.

Case 1: No noise

Using PVAF-1 (6), we can obtain the following theorem 1 for stability of the RZNN-1 model (8).

Theorem 1. If the solution of DSE in (1) exists, the state solution $X(t)$ of the RZNN-1 model (8) will converge to the theoretical solution $X^*(t)$ of DSE (1) within t_s for arbitrary initial system state.

$$t_s \le \frac{1}{\lambda a^k(pk-1)} + \frac{1}{\lambda b^k(1-qk)}.$$

Proof. According to (4), the evolution formula of the RZNN-1 model (8) can be written in the form of $\dfrac{\mathrm{d}E(t)}{\mathrm{d}t} = -\lambda\Gamma_1(E(t))$, and its n^2 subsystems can be obtained as:

$$\frac{\mathrm{d}e_{ij}(t)}{\mathrm{d}t} = -\lambda\tau(e_{ij}(t)) \quad i,j \in \{1,2,\ldots n\}. \tag{16}$$

where $e_{ij}(t)$ is the ij-th element of $E(t)$.

Consider the Lyapunov candidate function $v(t) = |e_{ij}(t)|$ for the DSE in (1). After substituting the PVAF-1 into the evolution formula, the derivative of $v(t)$ can be computed as:

$$\begin{aligned} \frac{\mathrm{d}v(t)}{\mathrm{d}t} &= \dot{e}_{ij}(t)\operatorname{sgn}(e_{ij}(t)) = -\lambda\tau(e_{ij}(t))\operatorname{sgn}(e_{ij}(t)) \\ &= -\lambda\Big(\left(a|e_{ij}(t)|^p + b|e_{ij}(t)|^q\right)^k \operatorname{sgn}(e_{ij}(t)) \\ &\quad + c_1 e_{ij}(t) + c_2\operatorname{sgn}(e_{ij}(t))\Big)\operatorname{sgn}(e_{ij}(t)) \\ &= -\lambda\left(\left(a|e_{ij}(t)|^p + b|e_{ij}(t)|^q\right)^k + c_1|e_{ij}(t)| + c_2\right) \\ &\le -\lambda\left(a|e_{ij}(t)|^p + b|e_{ij}(t)|^q\right)^k \\ &= -\left(\lambda^{1/k}\left(av^p(t) + bv^q(t)\right)\right)^k. \end{aligned}$$

According to Lemma 1, the following bounded convergent time t_{ij} of the ij-th subsystem can be obtained:

$$t_{ij} \le \frac{1}{\lambda a^k(pk-1)} + \frac{1}{\lambda b^k(1-qk)}.$$

Then the upper bound of the convergent time of the RZNN-1 model in (8) can be expressed as:

$$t_s = \max(t_{ij}) \leq \frac{1}{\lambda a^k(pk-1)} + \frac{1}{\lambda b^k(1-qk)}.$$

It can be noted that t_s is only dependent on some parameters of the system, which indicates that the RZNN-1 model (8) can achieve predefined time convergence in the situation without noise. □

Case 2: Attacked by DBDN

In the situation that the RZNN-1 model is attacked by DBDN, we can obtain the following Theorem 2 for stability of the RZNN-1 model in (10).

Theorem 2. If the solution of DSE (1) exists, the noise $N(t)$ in (10) is a DBDN, and $|n_{ij}(t)| \leq \delta|e_{ij}(t)|$ and $\lambda c_1 \geq \delta(\delta \in (0,+\infty))$ hold. The state solution $X(t)$ of the RZNN-1 model (10) can converge to the theoretical solution $X*(t)$ of DSE (1) within a predetermined time t_s for arbitrary initial system state.

$$t_s \leq \frac{1}{\lambda a^k(pk-1)} + \frac{1}{\lambda b^k(1-qk)}.$$

Proof. Differing from the above Theorem 1, the evolution formula of the RZNN-1 model (10) with noise can be written in the form of $\frac{\mathrm{d}E(t)}{\mathrm{d}t} = -\lambda\Gamma_1(E(t)) + N(t)$, and its n^2 subsystem can be obtained as:

$$\frac{\mathrm{d}e_{ij}(t)}{\mathrm{d}t} = -\lambda\tau_1(e_{ij}(t)) + n_{ij}(t) \quad i,j \in \{1,2,\ldots n\}. \tag{17}$$

where $n_{ij}(t)$ denotes the ij-th element of $N(t)$.

Consider the Lyapunov candidate function $v(t) = |e_{ij}(t)|^2$. Then, the time derivative of $v(t)$ can be computed as:

$$\frac{\mathrm{d}v(t)}{\mathrm{d}t} = 2e_{ij}(t)\dot{e}_{ij}(t) = 2e_{ij}(t)\left(-\lambda\tau_1\left(e_{ij}(t)\right) + n_{ij}(t)\right). \tag{18}$$

Based on PVAF-1 and the inequalities $|n_{ij}(t)| \leq \delta|e_{ij}(t)|$ and $\lambda c_1 \geq \delta$, we have:

$$\begin{aligned}
\frac{\mathrm{d}v(t)}{\mathrm{d}t} &= 2e_{ij}(t)\dot{e}_{ij}(t) = 2e_{ij}(t)\left(-\lambda\tau_1(e_{ij}(t)) + n_{ij}(t)\right) \\
&= 2e_{ij}(t)\Big(-\lambda\Big(\left(a\left|e_{ij}(t)\right|^p + b\left|e_{ij}(t)\right|^q\right)^k \mathrm{sgn}(e_{ij}(t)) \\
&\quad + c_1 e_{ij}(t) + c_2\mathrm{sgn}(e_{ij}(t))\Big) + n_{ij}(t)\Big) \\
&= -2\lambda\Big(\left(a\left|e_{ij}(t)\right|^p + b\left|e_{ij}(t)\right|^q\right)^k \left|e_{ij}(t)\right| \\
&\quad + c_1\left|e_{ij}(t)\right|^2 + c_2\left|e_{ij}(t)\right|\Big) + 2e_{ij}(t)n_{ij}(t) \\
&= -2\lambda\left(a\left|e_{ij}(t)\right|^{(p+1/k)} + b\left|e_{ij}(t)\right|^{(q+1/k)}\right)^k \\
&\quad + 2\left(e_{ij}(t)n_{ij}(t) - \lambda c_1\left|e_{ij}(t)\right|^2\right) - 2\lambda c_2\left|e_{ij}(t)\right| \\
&\leq -2\lambda\left(a\left|e_{ij}(t)\right|^{(p+1/k)} + b\left|e_{ij}(t)\right|^{(q+1/k)}\right)^k \\
&\quad + 2\left(\delta\left|e_{ij}(t)\right|^2 - \lambda c_1\left|e_{ij}(t)\right|^2\right) \\
&\leq -2\lambda\left(a\left|e_{ij}(t)\right|^{(p+1/k)} + b\left|e_{ij}(t)\right|^{(q+1/k)}\right)^k \\
&= -\left((2\lambda)^{(1/k)}\left(a\left|v_{ij}(t)\right|^{\left(\frac{pk+1}{2k}\right)} + b\left|v_{ij}(t)\right|^{\left(\frac{qk+1}{2k}\right)}\right)\right)^k.
\end{aligned}$$

According to Lemma 1, the following corresponding bounded convergent time t_{ij} of the ij-th subsystem can be obtained:

$$\begin{aligned}
t_{ij} &\leq \frac{1}{2\lambda a^k\left(\left(\frac{pk+1}{2k}\right)k - 1\right)} + \frac{1}{2\lambda b^k\left(1 - \left(\frac{qk+1}{2k}\right)k\right)} \\
&= \frac{1}{\lambda a^k(pk-1)} - \frac{1}{\lambda b^k(1-qk)}.
\end{aligned}$$

The upper bound convergent time of the RZNN-1 model (10) attacked by DBDN is obtained as:

$$t_s = \max(t_{ij}) \leq \frac{1}{\lambda a^k(pk-1)} - \frac{1}{\lambda b^k(1-qk)}.$$

Based on the above analysis, it can be observed that the RZNN-1 model under the attack of DBDN can obtain the solution of DSE in (1) within the predetermined time t_s. □

Case 3: Attacked by DBNDN

In the situation that the RZNN-1 model is attacked by DBNDN, we can obtain the following theorem 3 for stability of the RZNN-1 model in (10).

Theorem 3. If the solution of DSE (1) exists, the noise $N(t)$ in (10) is a DBNDN, and $|n_{ij}(t)| \leq \delta$ and $\lambda c_2 \geq \delta(\delta \in (0,+\infty))$ hold. The state solution $X(t)$ of the RZNN-1 model (10) can converge to the theoretical solution $X*(t)$ of DSE (1) within a predefined-time t_s for arbitrary initial system state.

$$t_s \leq \frac{1}{\lambda a^k(pk-1)} + \frac{1}{\lambda b^k(1-qk)}.$$

Proof. As done in Theorem 2, the evolution formula of the RZNN-1 model (10) can be written in the form of $\frac{\mathrm{d}E(t)}{\mathrm{d}t} = -\lambda\Gamma_1(E(t)) + N(t)$, and its n^2 subsystem can also be obtained as:

$$\frac{\mathrm{d}e_{ij}(t)}{\mathrm{d}t} = -\lambda\tau_1(e_{ij}(t)) + n_{ij}(t) \quad i,j \in \{1,2,\ldots n\}. \tag{19}$$

Consider the Lyapunov candidate $v(t) = |e_{ij}(t)|^2$. Then the time derivative of $v(t)$ can be expressed as:

$$\frac{\mathrm{d}v(t)}{\mathrm{d}t} = 2e_{ij}(t)\dot{e}_{ij}(t) = 2e_{ij}(t)\left(-\lambda\tau_1\left(e_{ij}(t)\right) + n_{ij}(t)\right). \tag{20}$$

Substituting PVAF-1 (6) and the inequalities $|n_{ij}(t)| \leq \delta$ and $\lambda c_2 \geq \delta$ into (20) results in:

$$\begin{aligned}
\frac{\mathrm{d}v(t)}{\mathrm{d}t} &= 2e_{ij}(t)\dot{e}_{ij}(t) = 2e_{ij}(t)\left(-\lambda\tau_1\left(e_{ij}(t)\right)+n_{ij}(t)\right) \\
&= 2e_{ij}(t)\Big(-\lambda\Big(\left(a\left|e_{ij}(t)\right|^p+b\left|e_{ij}(t)\right|^q\right)^k \mathrm{sgn}(e_{ij}(t)) \\
&\quad +c_1e_{ij}(t)+c_2\mathrm{sgn}(e_{ij}(t))\Big)+n_{ij}(t)\Big) \\
&= -2\lambda\Big(\left(a\left|e_{ij}(t)\right|^p+b\left|e_{ij}(t)\right|^q\right)^k\left|e_{ij}(t)\right|+c_1\left|e_{ij}(t)\right|^2 \\
&\quad +c_2\left|e_{ij}(t)\right|\Big)+2e_{ij}(t)n_{ij}(t) \\
&= -2\lambda\left(a\left|e_{ij}(t)\right|^{(p+1/k)}+b\left|e_{ij}(t)\right|^{(q+1/k)}\right)^k \\
&\quad +2\left(e_{ij}(t)n_{ij}(t)-\lambda c_2\left|e_{ij}(t)\right|\right)-2\lambda c_1\left|e_{ij}(t)\right|^2 \\
&\leq -2\lambda\left(a\left|e_{ij}(t)\right|^{(p+1/k)}+b\left|e_{ij}(t)\right|^{(q+1/k)}\right)^k \\
&\quad +2\left(\delta\left|e_{ij}(t)\right|-\lambda c_2\left|e_{ij}(t)\right|\right) \\
&\leq -2\lambda\left(a\left|e_{ij}(t)\right|^{(p+1/k)}+b\left|e_{ij}(t)\right|^{(q+1/k)}\right)^k \\
&= -\left((2\lambda)^{(1/k)}\left(a\left|v_{ij}(t)\right|^{\left(\frac{pk+1}{2k}\right)}+b\left|v_{ij}(t)\right|^{\left(\frac{qk+1}{2k}\right)}\right)\right)^k.
\end{aligned}$$

According to Lemma 1, it can be found that the bounded convergent time t_{ij} of the ij-th subsystem is:

$$\begin{aligned}
t_{ij} &\leq \frac{1}{2\lambda a^k\left(\left(\frac{pk+1}{2k}\right)k-1\right)}+\frac{1}{2\lambda b^k\left(1-(\frac{qk+1}{2k})k\right)} \\
&= \frac{1}{\lambda a^k(pk-1)}+\frac{1}{\lambda b^k(1-qk)}.
\end{aligned}$$

The upper bound convergent time of the RZNN-1 model (10) attacked by DBNDN is obtained.

$$t_s = \max(t_{ij}) \leq \frac{1}{\lambda a^k(pk-1)}+\frac{1}{\lambda b^k(1-qk)}.$$

Based on the above results, it can be observed that the RZNN-1 model (10) under the attack of DBNDN can obtain the solution of DSE in (1) within predetermined time t_s. □

4.2. RZNN-2 model analysis

In this section, the stability of RZNN-2 in various cases will be demonstrated.

Case 1: No noise

Using PVAF-2 (7), we can obtain the following theorem 4 for stability of the RZNN-2 model (9).

Theorem 4. If the solution of DSE in (1) exists, the state solution $X(t)$ of the RZNN-2 model (9) will converge to the theoretical solution $X*(t)$ of DSE (1) within t_s for arbitrary initial system state.

$$t_s \leq \frac{1}{\lambda b^k}\left(\frac{b}{a}\right)^{(1/p)}\left(1+\frac{1}{pk-1}\right).$$

Proof. According to (4), the evolution formula of the RZNN-2 model (9) can be written in the form of $\frac{\mathrm{d}E(t)}{\mathrm{d}t} = -\lambda\Gamma_1(E(t))$, and its n^2 subsystems can be obtained as:

$$\frac{\mathrm{d}e_{ij}(t)}{\mathrm{d}t} = -\lambda\tau_2\left(e_{ij}(t)\right) \quad i,j\in\{1,2,\ldots n\}. \tag{21}$$

Consider the Lyapunov candidate function $v(t) = |e_{ij}(t)|$ for the DSE in (1). After substituting PVAF-2 into the evolution formula (21), the derivative of $v(t)$ can be computed as:

$$\begin{aligned}
\frac{\mathrm{d}v(t)}{\mathrm{d}t} &= \dot{e}_{ij}(t)\mathrm{sgn}\left(e_{ij}(t)\right) = -\lambda\tau_2\left(e_{ij}(t)\right)\mathrm{sgn}\left(e_{ij}(t)\right) \\
&= -\lambda\Big(\left(a\left|e_{ij}(t)\right|^p+b\right)^k\mathrm{sgn}(e_{ij}(t))+d_1e_{ij}(t) \\
&\quad +d_2\mathrm{sgn}(e_{ij}(t))\Big)\mathrm{sgn}\left(e_{ij}(t)\right) \\
&= -\lambda\left(\left(a\left|e_{ij}(t)\right|^p+b\right)^k+d_1\left|e_{ij}(t)\right|+d_2\right) \\
&\leq -\lambda\left(a\left|e_{ij}(t)\right|^p+b\right)^k = -\left(\lambda^{(1/k)}\left(av^p(t)+b\right)\right)^k.
\end{aligned}$$

According to Lemma 2, the corresponding bounded convergent time t_{ij} of the ij-th subsystem can be obtained:

$$t_{ij} \leq \frac{1}{\lambda b^k}\left(\frac{b}{a}\right)^{(1/p)}\left(1+\frac{1}{pk-1}\right).$$

Then the upper bound of the convergent time of the RZNN-2 model in (9) can be expressed as:

$$t_s = \max(t_{ij}) \leq \frac{1}{\lambda b^k}\left(\frac{b}{a}\right)^{(1/p)}\left(1+\frac{1}{pk-1}\right).$$

It can be noted that t_s is only dependent on some parameters of the system, which indicates that the RZNN-1 model (8) achieves predefined-time convergence in the situation without noise. □

Case 2: Attacked by DBDN

In the situation that the RZNN-2 model is attacked by DBDN, we can obtain the following Theorem 5 for stability of the RZNN-2 model in (11).

Theorem 5. If the solution of DSE (1) exists, the noise $N(t)$ in (11) is a DBDN, and $|n_{ij}(t)| \leq \delta|e_{ij}(t)|$ and $\lambda d_1 \geq \delta(\delta \in (0,+\infty))$ hold. The state solution $X(t)$ of RZNN-2 model (11) can converge to the theoretical solution $X*(t)$ of DSE (1) within a predetermined time t_s for arbitrary initial system state.

$$t_s \leq \frac{1}{\lambda b^k}\left(\frac{b}{a}\right)^{(1/p)}\left(1+\frac{1}{pk-1}\right).$$

Proof. The evolution formula of the RZNN-2 model (11) with noise can be written in the form of $\frac{\mathrm{d}E(t)}{\mathrm{d}t} = -\lambda\Gamma_1(E(t))+N(t)$, and its n^2 subsystem can be obtained as:

$$\frac{\mathrm{d}e_{ij}(t)}{\mathrm{d}t} = -\lambda\tau_2(e_{ij}(t))+n_{ij}(t) \quad i,j\in\{1,2,\ldots n\}. \tag{22}$$

Consider the Lyapunov candidate function $v(t) = |e_{ij}(t)|$. Then, the time derivative of $v(t)$ can be computed as:

$$\begin{aligned}\frac{\mathrm{d}v(t)}{\mathrm{d}t} &= \dot{e}_{ij}(t)\mathrm{sgn}(e_{ij}(t)) \\ &= (-\lambda\tau_2(e_{ij}(t)) + n_{ij}(t))\,\mathrm{sgn}(e_{ij}(t)).\end{aligned} \tag{23}$$

Based on PVAF-2 and the inequalities $|n_{ij}(t)| \le \delta|e_{ij}(t)|$ and $\lambda d_1 \ge \delta$, we have:

$$\begin{aligned}\frac{\mathrm{d}v(t)}{\mathrm{d}t} &= \dot{e}_{ij}(t)\mathrm{sgn}(e_{ij}(t)) = (-\lambda\tau_2(e_{ij}(t)) + n_{ij}(t))\,\mathrm{sgn}(e_{ij}(t)) \\ &= \Big(-\lambda\Big(\big(a|e_{ij}(t)|^p + b\big)^k \mathrm{sgn}(e_{ij}(t)) + d_1 e_{ij}(t) \\ &\quad + d_2\mathrm{sgn}(e_{ij}(t))\Big) + n_{ij}(t)\Big)\mathrm{sgn}(e_{ij}(t)) \\ &= -\lambda\left(a|e_{ij}(t)|^p + b\right)^k - \lambda d_1|e_{ij}(t)| \\ &\quad - \lambda d_2 + n_{ij}(t)\mathrm{sgn}(e_{ij}(t)) \\ &\le -\lambda\left(a|e_{ij}(t)|^p + b\right)^k + \left(\delta|e_{ij}(t)| - \lambda d_1|e_{ij}(t)|\right) \\ &\le -\lambda\left(a|e_{ij}(t)|^p + b\right)^k = -\left(\lambda^{(1/k)}(av^p(t) + b)\right)^k.\end{aligned}$$

According to Lemma 2, the corresponding bounded convergent time t_{ij} of the ij-th subsystem is:

$$t_{ij} \le \frac{1}{\lambda b^k}\left(\frac{b}{a}\right)^{(1/p)}\left(1 + \frac{1}{pk-1}\right).$$

The upper bound convergent time of the RZNN-2 model (11) attacked by DBDN is obtained as:

$$t_s = \max(t_{ij}) \le \frac{1}{\lambda b^k}\left(\frac{b}{a}\right)^{(1/p)}\left(1 + \frac{1}{pk-1}\right).$$

Based on the above analysis, it can be observed that the RZNN-2 model under the attack of DBDN can obtain the solution of DSE in (1) within the predefined-time t_s. □

Case 3: Attacked by DBNDN

In the situation that the RZNN-2 model is attacked by DBNDN, we can obtain the following theorem 6 for stability of the RZNN-2 model in (11).

Theorem 6. If the solution of DSE (1) exists, the noise $N(t)$ in (11) is a DBNDN, and $|n_{ij}(t)| \le \delta$ and $\lambda d_2 \ge \delta(\delta \in (0, +\infty))$ hold. The state solution $X(t)$ of RZNN-1 model (10) can converge to the theoretical solution $X*(t)$ of DSE (1) within a predetermined time t_s for arbitrary initial system state.

$$t_s \le \frac{1}{\lambda b^k}\left(\frac{b}{a}\right)^{(1/p)}\left(1 + \frac{1}{pk-1}\right).$$

Proof. As done in Theorem 5, the evolution formula of the RZNN-2 model (11) can be written in the form of $\frac{\mathrm{d}E(t)}{\mathrm{d}t} = -\lambda\Gamma_1(E(t)) + N(t)$, and its n^2 subsystem can also be obtained as:

$$\frac{\mathrm{d}e_{ij}(t)}{\mathrm{d}t} = -\lambda\tau_2(e_{ij}(t)) + n_{ij}(t) \quad i, j \in \{1, 2, \ldots n\}. \tag{24}$$

Consider the Lyapunov candidate $v(t) = |e_{ij}(t)|$. Then the time derivative of $v(t)$ can be expressed as:

$$\begin{aligned}\frac{\mathrm{d}v(t)}{\mathrm{d}t} &= \dot{e}_{ij}(t)\mathrm{sgn}\left(e_{ij}(t)\right) \\ &= \left(-\lambda\tau_2\left(e_{ij}(t)\right) + n_{ij}(t)\right)\mathrm{sgn}(e_{ij}(t)).\end{aligned} \tag{25}$$

Substituting PVAF-2 (7) and the inequalities $|n_{ij}(t)| \le \delta$ and $\lambda d_2 \ge \delta$ into (25) results in:

$$\begin{aligned}\frac{\mathrm{d}v(t)}{\mathrm{d}t} &= \dot{e}_{ij}(t)\mathrm{sgn}\left(e_{ij}(t)\right) = \left(-\lambda\tau_2\left(e_{ij}(t)\right) + n_{ij}(t)\right)\mathrm{sgn}(e_{ij}(t)) \\ &= \Big(-\lambda\Big(\left(a|e_{ij}(t)|^p + b\right)^k \mathrm{sgn}(e_{ij}(t)) + d_1 e_{ij}(t) \\ &\quad + d_2\mathrm{sgn}(e_{ij}(t))\Big) + n_{ij}(t)\Big)\mathrm{sgn}\left(e_{ij}(t)\right) \\ &= -\lambda\left(a|e_{ij}(t)|^p + b\right)^k - \lambda d_1|e_{ij}(t)| \\ &\quad - \lambda d_2 + n_{ij}(t)\mathrm{sgn}\left(e_{ij}(t)\right) \\ &\le -\lambda\left(a|e_{ij}(t)|^p + b\right)^k + (\delta - \lambda d) \\ &\le -\lambda\left(a|e_{ij}(t)|^p + b\right)^k = -\left(\lambda^{(1/k)}(av^p(t) + b)\right)^k.\end{aligned}$$

According to Lemma 2, it can be found that the corresponding bounded convergent time t_{ij} of the ij-th subsystem is:

$$t_{ij} \le \frac{1}{\lambda b^k}\left(\frac{b}{a}\right)^{(1/p)}\left(1 + \frac{1}{pk-1}\right).$$

The upper bound convergent time of the RZNN-2 model (10) attacked by DBNDN is obtained as:

$$t_s = \max(t_{ij}) \le \frac{1}{\lambda b^k}\left(\frac{b}{a}\right)^{(1/p)}\left(1 + \frac{1}{pk-1}\right).$$

Based on the above results, it can be observed that the RZNN-2 model (11) under the attack of DBNDN can obtain the solution of DSE in (1) within predetermined time t_s. □

Combining Theorems 1–6, it can be concluded that the two proposed RZNN models (PVAF-1 activated RZNN-1 and PVAF-2 activated RZNN-2) converge to the theoretical solution of DSE (1) within fixed-time and they are robust to noise.

5. NUMERICAL SIMULATION VERIFICATION

In this section, numerical examples are carried out to verify their effectiveness in calculating the solution of DSE (1). In this section, a comparison with the SBPAF-activated ZNN model (5) in Table 1 is also conducted.

The proposed RZNN models activated by the two new PVAFs in Table 2 are applied to solve the DSE (1). In addition, recently reported AFs and the proposed PVAFs are listed in Table 2. Based on Table 2, it can be observed that all the AFs have differences in their structure, which leads to different performance of the ZNN models.

It is worth pointing out that the variable k in PVAF-1 and PVAF-2 is a parameter designed by the user, and the VAF in Table 1 is a special case of the new proposed PVAF-1 with $k = 1$.

Table 2
Recently reported AFs and proposed PVAFs

Models	Activation functions
ZNN in [35]	$n(x)=(\alpha_1\lvert x\rvert^{\rho}+\alpha_2\lvert x\rvert^{\varphi})^{s}\operatorname{sgn}(x)+\alpha_3\exp\left(\lvert x\rvert^{\lambda}\right)\lvert x\rvert^{\lambda-1}\operatorname{sgn}(x)/\lambda+\alpha_4\operatorname{sgn}(x)$
RFCZNN in [36]	$\varphi(x)=\operatorname{sgn}^{p/q}(x)+\operatorname{sgn}^{q/p}(x)+k_1x+k_2\operatorname{sgn}(x)$
BFCZNN in [37]	$\phi(x)=w_1\exp(\lvert x\rvert^{p})\lvert x\rvert^{1-p}\operatorname{sgn}(x)/p+\left(w_2\lvert x\rvert^{q}+w_3\lvert x\rvert^{1/q}\right)\operatorname{sgn}(x)$
RZNN in this work	$\tau_1(x)=(a\lvert x\rvert^{p}+b\lvert x\rvert^{q})^{k}\operatorname{sgn}(x)+c_1x+c_2\operatorname{sgn}(x)$
	$\tau_2(x)=(a\lvert x\rvert^{p}+b)^{k}\operatorname{sgn}(x)+d_1x+d_2\operatorname{sgn}(x)$

The dynamic coefficient matrices of DSE (1) are given below.

$$D=\begin{pmatrix}\sin 3t & \cos 3t & \sin t\\ -\cos 3t & \sin 3t & \cos t\\ -\sin t & -\cos 2t & \sin 3t\end{pmatrix},$$

$$G=\begin{pmatrix}20 & 0 & 10\\ 0 & 30 & 0\\ 0 & 15 & 20\end{pmatrix},$$

$$M=\begin{pmatrix}\sin 3t & \cos 3t & \sin t\\ -\cos 3t & \sin 3t & \cos t\\ \sin t & \cos t & \sin 3t\end{pmatrix}.$$

For arbitrary initial system state, the RZNN-1 and RZNN-2 models activated by the PVAF-1 and PVAF-2 with $k=0.5$, $k=1$ and $k=2$ are applied to compute the solution of DSE (1) under the attack of the four noises which are given in Table 3.

Table 3
Noises

No.	Noise item	Expression
1	Periodic noise (PN)	$n(t)=1.5\cos(t)$
2	Constant noise (CN)	$n(t)=1.5$
3	Non-disappearing noise (NDN)	$n(t)=0.1t$
4	Disappearing noise (DN)	$n(t)=\exp(-t)$

The state solutions of DSE (1) obtained by the RZNN-1 model (10) with $k=0.5,1,2$ under the attack of PN $n(t)=1.5\cos(t)$ are presented in Fig. 1(a–c), respectively. The red dotted curves and blue solid curves represent the theoretical solutions of DSE (1) and the state solutions obtained by the RZNN-1 model (10), respectively. As shown in Fig. 1(a–c), the RZNN-1 model (10) activated by the PVAF-1 solves DSE (1) quickly and robustly. Moreover, we can observe that the convergent performance of the RZNN-1 model (10) improves as the value of k increases.

The neutral state solutions of DSE (1) solved by the ZNN model (5) activated by SBPAF in Table 1 is presented in Fig. 1(d), from which it can be observed that the ZNN model (5) cannot accurately solve DSE (1) under the attack of PN $n(t)=1.5\cos(t)$.

The residual errors $\|D(t)X(t)-X(t)G(t)+M(t)\|_F$ of the RZNN-1 model (10) activated by the PVAF-1 and the ZNN model (5) activated by the SBPAF are illustrated in Fig. 2 and Fig. 3, from which it can be observed that the RZNN-1 model (10) solves DSE (1) under the attack of various noises, while the ZNN model (5) activated by the SBPAF fails. Additionally, it also can be observed that the convergent speed of RZNN-1 model (10) is dependent on parameter k, which means that the convergent rate of the RZNN-1 model can be adjusted by choosing an appropriate k.

The state solutions of DSE (1) obtained by RZNN-2 model (11) with $k=0.5$, $k=1$, $k=2$ under the attack of PN $n(t)=1.5\cos(t)$ are described in Fig. 4(a–c), respectively, from which it can be observed that the RZNN-2 model (11) activated by the PVAF-2 also solves DSE (1) quickly and robustly. Moreover, it also can be seen that the convergent performance of the RZNN-2 model (11) improves as the value of k increases. The corresponding residual errors of RZNN-2 and ZNN activated by SBPAF with PN $n(t)=1.5\cos(t)$ is presented in Fig. 4(d).

The residual errors $\|D(t)X(t)-X(t)G(t)+M(t)\|_F$ of the RZNN-2 model (11) activated by the PVAF-2 with $k=0.5,1,2$ and the ZNN model (5) activated by the SBPAF for solving DSE (1) are shown in Fig. 5 and Fig. 6, which show that the RZNN-2 model (11) solves DSE (1) effectively in noise-polluted environment. It can be observed that the proposed RZNN-2 model (11) has better performance than the ZNN model (5) in noisy environment. Moreover, it also can be observed that the convergent speed of the RZNN-2 model (11) is dependent on parameter k. Specifically, the convergence and anti-noise performance of the RZNN-2 model (11) become better as k increases, which means that the convergent rate of the RZNN-2 model can be adjusted by choosing an appropriate k.

Remark 1. Parameter k is the key technique of the two proposed new PVAFs, and the convergence and robustness of the RZNN models become better as k increases. Although it should be better to choose a large k, the choice of k may be constrained by some hardware conditions, such as the value of capacitance, inductance or diodes. Thus, it needs a tradeoff between performance and hardware in practical applications.

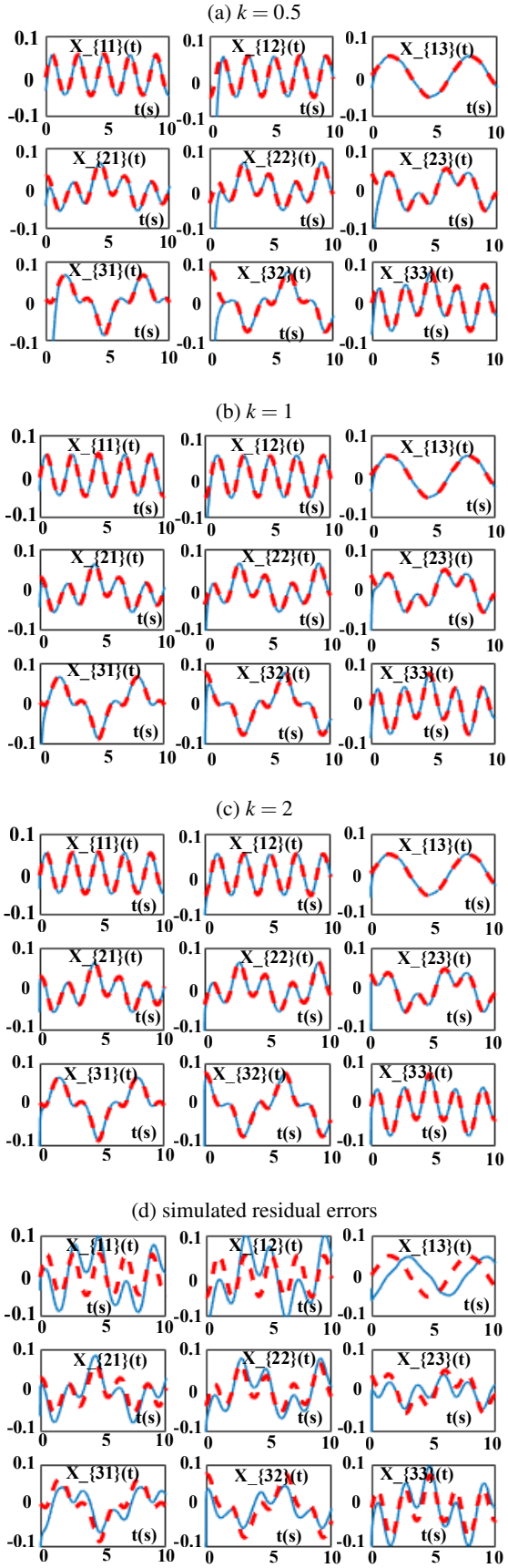

Fig. 1. (a–c) Solved by the RZNN-1 model with PN $n(t) = 1.5\cos(t)$ and (d) solved by ZNN model (5) activated by SBPAF with PN $n(t) = 1.5\cos(t)$

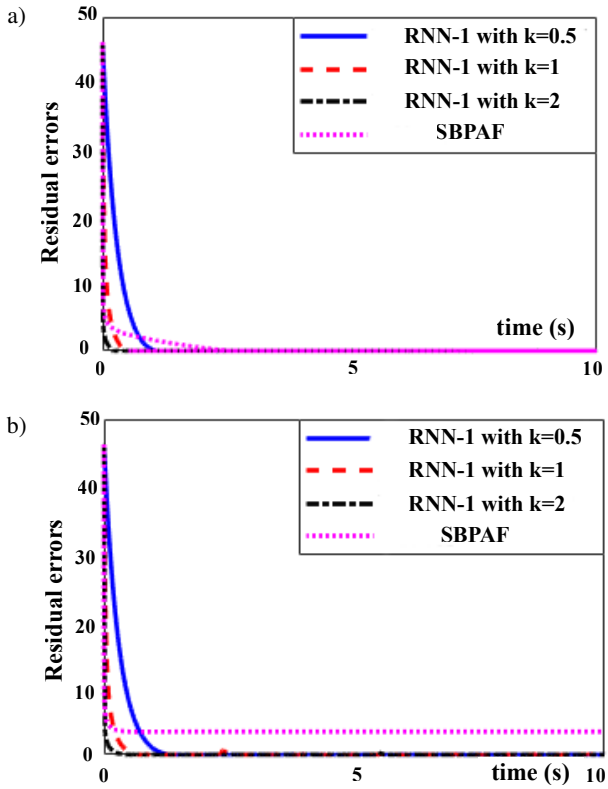

Fig. 2. Residual errors of RZNN-1 and ZNN activated by SBPAF a) without noise and b) with CN $n(t) = 1.5$

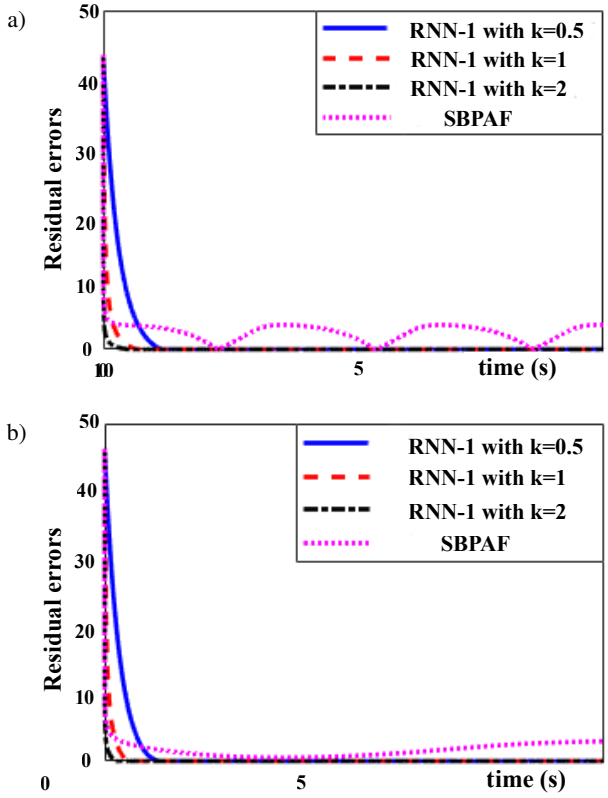

Fig. 3. Residual errors of RZNN-1 and ZNN activated by SBPAF a) with PN $n(t) = 1.5\cos(t)$ and b) with NDN $n(t) = 0.1t$

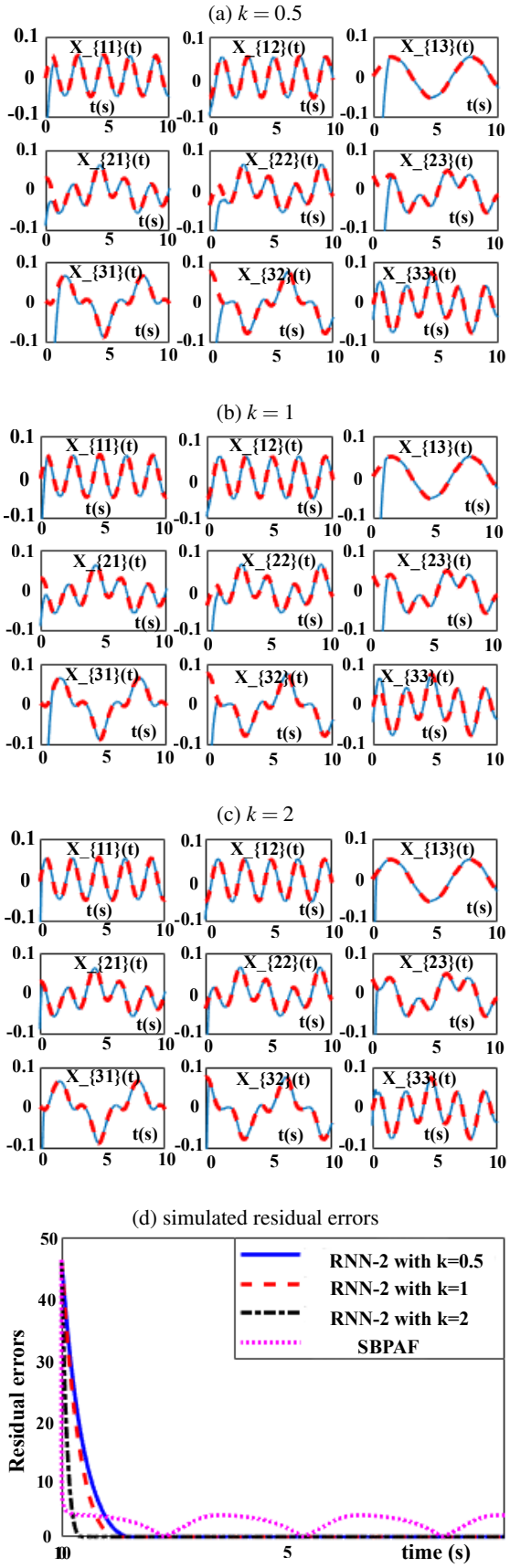

Fig. 4. (a–c). Solved by the RZNN-2 model with PN $n(t) = 1.5\cos(t)$ and (d) residual errors of RZNN-2 and ZNN activated by SBPAF with PN $n(t) = 1.5\cos(t)$

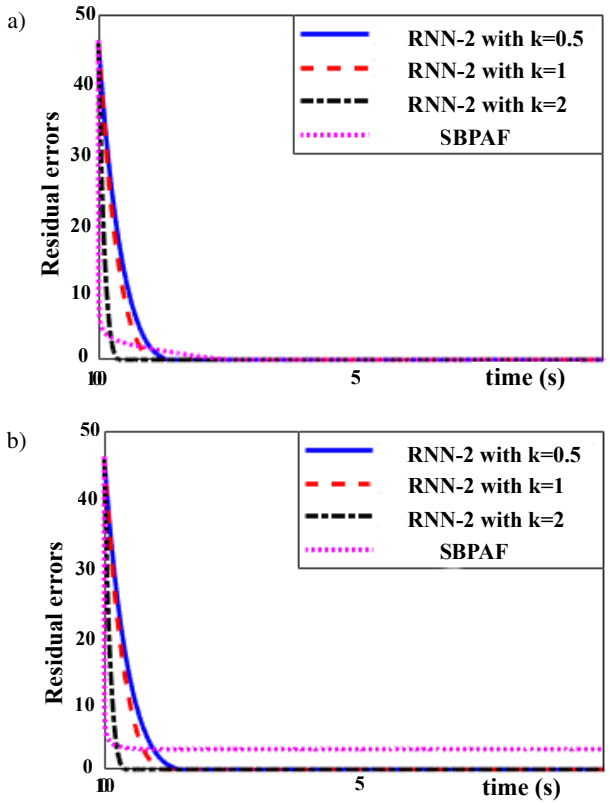

Fig. 5. Simulated residual errors of RZNN-2 and SBPAF-based ZNN a) without noise and b) with CN $n(t) = 1.5$

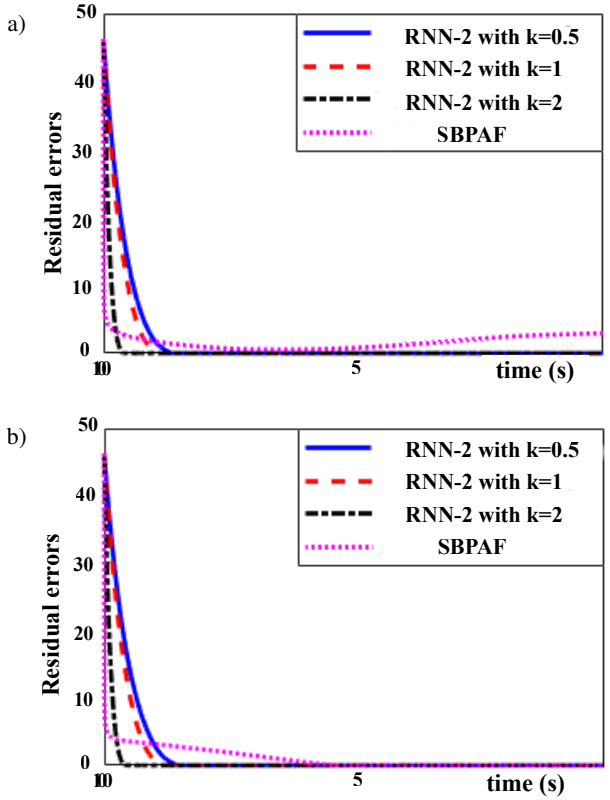

Fig. 6. Simulated residual errors of RZNN-2 and SBPAF-based ZNN a) with NDN $n(t) = 0.1t$ and b) with DN $n(t) = \exp(-t)$

6. APPLICATION OF MECHANICAL ARM

With the development of artificial intelligence, intelligent circuits [ ] and robots have become a hot research topic in recent years [38–43]. In this section, the RZNN-2 model is applied to control the robotic manipulator to track a given trajectory under the attack of constant noise. Additionally, a comparison with a SBPAF-based ZNN model is conducted.

The kinematic model of an MRM is described below [44, 45].

$$r(t) = \xi(\theta(t)), \tag{26}$$

where $r(t)$ represents the position of the end-effector, $\theta(t)$ denotes the joint angle and $\xi(\cdot)$ is a nonlinear function. The motion equation of the velocity level is:

$$\dot{r}(t) = J(\theta)\dot{\theta}(t), \tag{27}$$

where $J(\theta) = \dfrac{\partial \xi(\theta)}{\partial \theta}$ is the Jacobian matrix.

The control objective is to design control law $\mu = \dot{\theta}$, such that the tracking error $e(t) = r(t) - r_d(t)$ converges to 0 within predefined time in noisy environment, where $r_d(t)$ is the reference trajectory. To achieve such an objective, the proposed RZNN-2 model (11) and the SBPAF-based ZNN model (5) are applied to design the control law, respectively. The kinematic control models to generate control input are shown as follows.

$$J\dot{\mu} = -\dot{J}\theta + \ddot{r}_d - \lambda\Gamma_2(J\mu - \dot{r}_d) + n(t), \tag{28}$$

$$J\dot{\mu} = -\dot{J}\theta + \ddot{r} - \lambda\Gamma(J\mu - \dot{r}_d) + n(t). \tag{29}$$

Equations (28) and (29) are the kinematic control models of the MRM when the RZNN-2 model (11) and SBPAF-activated ZNN model (5) are used, respectively.

The RZNN-based model (28) is used for the MRM to perform task tracking of a windmill under the condition of CN $n(t) = 0.5$, and the simulation results are presented in Fig. 7. Figure 7(a) is the tracking trajectory of the MRM, Fig. 7(b) is the desired path and actual trajectory of the MRM, and Fig. 7(c) is the tracking error of the MRM based on (28). As seen from Fig. 7, the MRM based on (28) completes the windmill-shaped tracking task successfully, and the actual tracking trajectory of the MRM matches the desired path exactly.

Then, the ZNN-based model (5) activated by SBPAF is also used for the MRM to complete the same task under the same condition, and the related simulation results are shown in Fig. 8. We can observe from Fig. 8 that owing to the influence of additive CN $n(t) = 0.5$, the actual tracking trajectory of the MRM cannot coincide with the expected windmill-shaped path. In other words, the MRM based on (29) fails to accomplish the tracking task of a windmill-shaped path owing to the additive interference.

A six-joint manipulator is driven to track a circle with radius $r = 5$ cm by using the RZNN-based model (28). The simulated results are presented in Fig. 9, which further verifies effectiveness of the proposed RZNN models.

A real robotic manipulator is also used to further validate the correctness and effectiveness of the RZNN-based model (28).

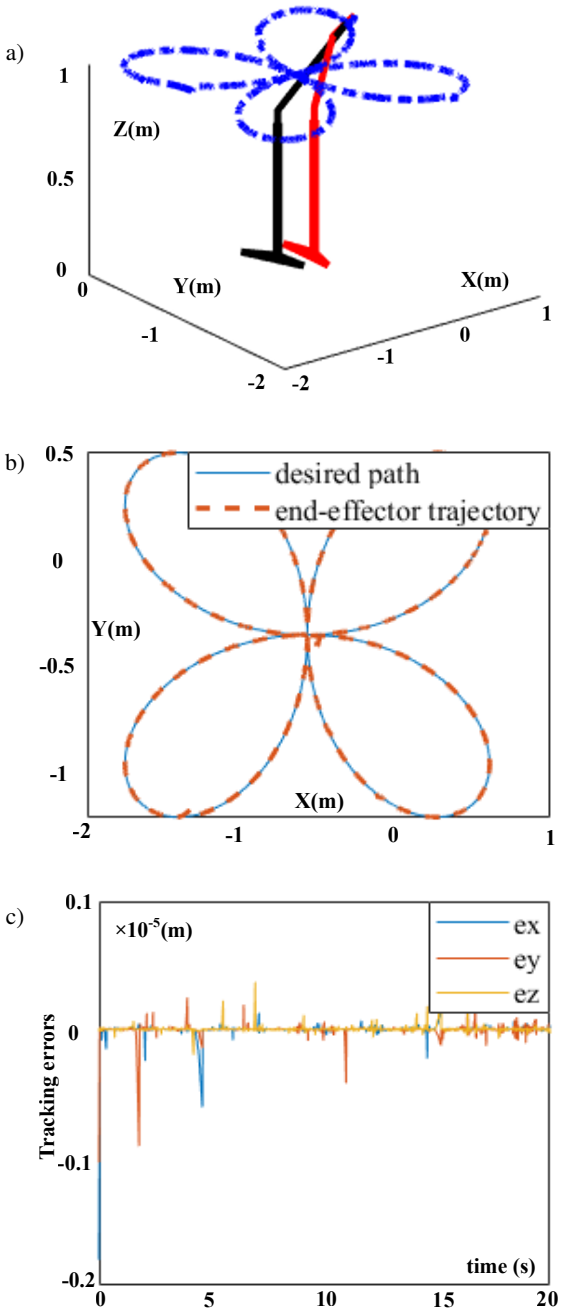

Fig. 7. Trajectory tracking results of MRM synthesized by RZNN-2 with $n(t) = 0.05$. (a) Top view of the tracking trajectory. (b) Actual trajectory and desired tracking path. (c) Tracking errors. (ex, ey and ez in (c) are the position errors between the desired path and the end-effector trajectory in X, Y and Z directions, respectively)

The desired task of the real robotic manipulator is also to track a circle with radius $r = 5$ cm. In this physical experiments, the snapshots during the completion of the circle tracking task synthesized by the RZNN-based model (28) are presented in Fig. 10. It can be observed from Fig. 10 that the real robotic manipulator synthesized by the RZNN-based model (28) fulfills the circle tracking task successfully, which further verifies the practicality and effectiveness of the proposed RZNN models.

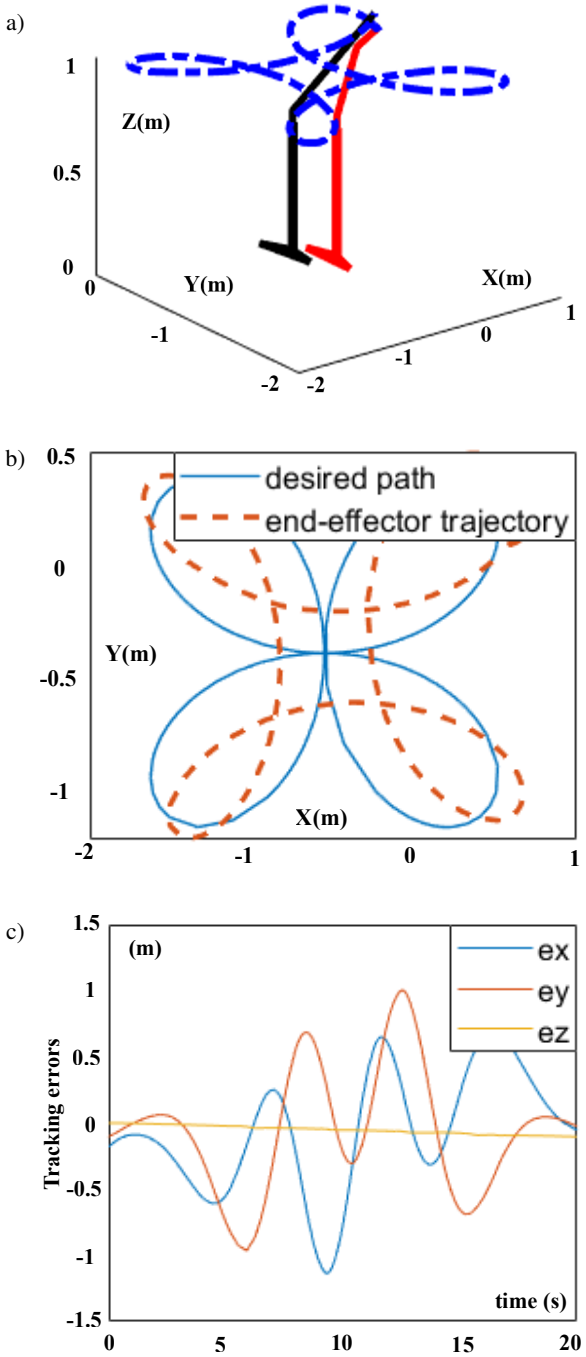

Fig. 8. Trajectory tracking results of MRM synthesized by SBPAF-based ZNN with $n(t) = 0.5$. a) Top view of the tracking trajectory. b) Actual trajectory and desired tracking path. c) Tracking errors. (ex, ey and ez in (c) are the position errors between the desired path and the end-effector trajectory in X, Y and Z directions, respectively)

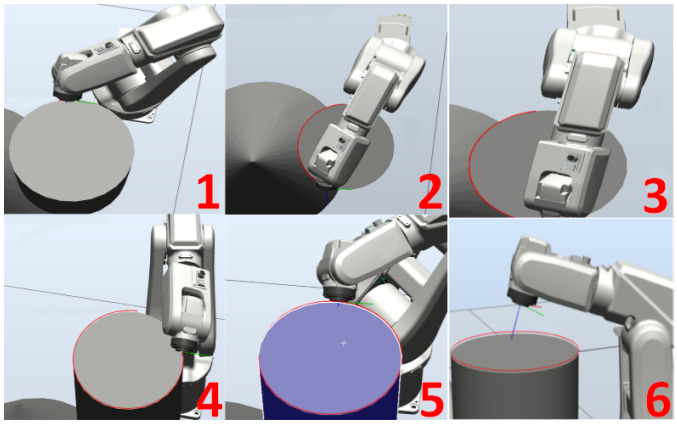

Fig. 9. Simulated circle tracking experiments synthesized by the RZNN-based model (28)

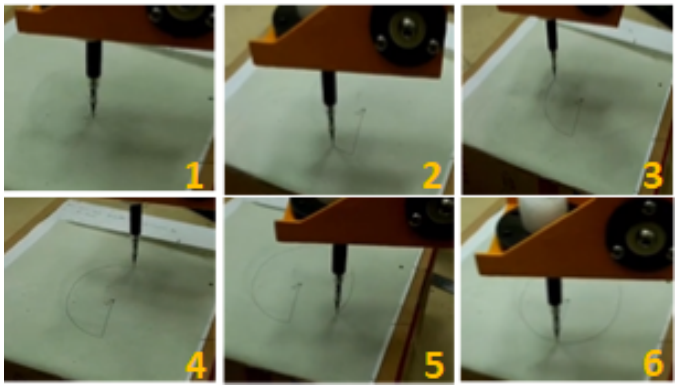

Fig. 10. Physical circle tracking experiments synthesized by the RZNN-based model (28)

7. CONCLUSIONS

In this paper, the main contribution lies in the design of two new PVAFs. Then, two RZNN models for solving DSE are constructed by employing these two activation functions. Compared with the existing ZNN models, the proposed two models have significant advantages in fixed-time convergence and anti-jamming capability. In order to verify their unique advantages, we first prove strictly from mathematical analysis. Then, similarly to theoretical analysis, noises are also taken into consideration in the simulation experiments. The experimental results are consistent with theoretical discussion, which further emphasizes reliability of the RZNN models. Future research directions could be focused on improvement of the structure of the existing ZNN model and the expanded applications of the RZNN models in practical engineering problems.

DATA AVAILABILITY

All the data and code used to support the findings in this study are available from the corresponding authors upon request (Mingtao Tan and Peng Zhou, e-mail: lightsdu@sina.cn and zhoupeng@guat.edu.cn).

ACKNOWLEDGEMENTS

This work was supported by the Guiding Plan Project of Scientific and Technological Innovation and Development in Changde (Grant/Award Number: 2020ZD37), and also supported by the scientific research project from Hunan University of Arts and Science (Grant/Award Number: 21ZD03).

REFERENCES

[1] A. Benzaouia, M. Ait Rami, and S. El Faiz, "Stabilization of linear systems with saturation: a Sylvester equation approach", *IMA J. Math. Control Inf.*, vol. 21, no. 3, pp. 247–259, Sept. 2004.

[2] Q. Wei, N. Dobigeon, and J. Tourneret, "Fast Fusion of Multi-Band Images Based on Solving a Sylvester Equation," *IEEE Trans. Image Process.*, vol. 24, no. 11, pp. 4109–4121, Nov. 2015.

[3] Q. Wei, N. Dobigeon, J. Tourneret, J. Bioucas-Dias, and S. Godsill, "R-FUSE: Robust Fast Fusion of Multiband Images Based on Solving a Sylvester Equation," *IEEE Signal Process. Lett.*, vol. 23, no. 11, pp. 1632–1636, Nov. 2016.

[4] V.L. Syrmos, "Disturbance decoupling using constrained Sylvester equations," *IEEE Trans. Autom. Control*, vol. 39, no. 4, pp. 797–803, April 1994.

[5] W. Zhang and D. Zhou, "Coupled iterative algorithms based on optimisation for solving Sylvester matrix equations," *IET Contr. Theory Appl.*, vol. 13, no. 4, pp. 584–593, 2019.

[6] A. Wu and G. Duan, "Solution to the generalised sylvester matrix equation AV + BW = AVF," *IET Contr. Theory Appl.*, vol. 1, no. 1, pp. 402–408, January 2007.

[7] G.R. Duan, "On the solution to the Sylvester matrix equation AV+BW=EVF," *IEEE Trans. Autom. Control*, vol. 41, no. 4, pp. 612–614, April 1996.

[8] M. Dehghan, and M. Hajarian, "Efficient iterative method for solving the second-order Sylvester matrix equation EVF2-AVF-CV=BW," *IET Contr. Theory Appl.*, vol. 3, no. 10, pp. 1401–1408, October 2009.

[9] G.R. Duan and B, Zhou, "Solution to the second-order Sylvester matrix equation MVF/sup 2/+DVF+KV=BW," *IEEE Trans. Autom. Control*, vol. 51, no. 5, pp. 805–809, 2006.

[10] A. Wu, G. Duan, and Y. Xue, "Kronecker Maps and Sylvester-Polynomial Matrix Equations," *IEEE Trans. Autom. Control*, vol. 52, no. 5, pp. 905–910, May 2007.

[11] Y. Lin, L. Bao, and Y. Wei, "Matrix Sign Function Methods for Solving Projected Generalized Continuous-Time Sylvester Equations," *IEEE Trans. Autom. Control*, vol. 55, no. 11, pp. 2629–2634, Nov. 2010.

[12] F. Ding and T. Chen, "Gradient based iterative algorithms for solving a class of matrix equations," *IEEE Trans. Autom. Control*, vol. 50, no. 8, pp. 1216–1221, Aug. 2005.

[13] Z. Huamin, "Gradient-based iterative algorithm for the extended coupled Sylvester matrix equations," *2017 29th Chinese Control and Decision Conference (CCDC)*, Chongqing, 2017, pp. 1562–1567.

[14] J. Zhu, J. Jin, W. Chen, and J, Gong, "A combined power activation function based convergent factor-variable ZNN model for solving dynamic matrix inversion," *Math. Comput. Simul.*, vol. 197, pp. 291–307, 2022.

[15] J. Jin, "An Improved Finite Time Convergence Recurrent Neural Network with Application to Time-Varying Linear Complex Matrix Equation Solution," *Neural Process. Lett.*, vol. 53, pp. 777–786, 2021.

[16] J. Jin, L. Xiao, M. Lu, and J. Li, "Design and Analysis of Two FTRNN Models With Application to Time-Varying Sylvester Equation," *IEEE Access*, vol. 7, pp. 58945–58950, 2019.

[17] F. Yu, L. Liu, L. Xiao, K. Li, and S. Cai, "A robust and fixed-time zeroing neural dynamics for computing time-variant nonlinear equation using a novel nonlinear activation function," *Neurocomputing*, vol. 350, pp. 108–116, 2019.

[18] J.H. Mathews and K.D. Fink, *Numerical methods using MATLAB. Englewood Cliffs*, NJ, USA: Prentice-Hall, 2004.

[19] Y. Zhang and H.F. Peng, "Zhang Neural Network for Linear Time-Varying Equation Solving and its Robotic Application," *2007 International Conference on Machine Learning and Cybernetics*, pp. 3543–3548 2007.

[20] Y. Zhang, K. Chen, X. Li, C. Yi, and H. Zhu, "Simulink modeling and comparison of Zhang Neural Networks, and gradient Neural Networks, for time-varying Lyapunov equation solving," *Proceedings of IEEE International Conference on Natural Computation*, vol. 3, pp. 521–525, 2008.

[21] W. Li, L. Xiao, and B. Liao, "A Finite-Time Convergent and Noise-Rejection Recurrent Neural Network and Its Discretization for Dynamic Nonlinear Equations Solving," *IEEE Trans. Cybern.*, vol. 50, no. 7, pp. 3195–3207, 2020.

[22] Z. Zhang, Z. Li, and S. Yang, "A Barrier Varying-Parameter Dynamic Learning Network for Solving Time-Varying Quadratic Programming Problems with Multiple Constraints," *IEEE Trans. Cybern.*, doi: 10.1109/TCYB.2021.3051261.

[23] S. Li, S. Chen, and B. Liu, "Accelerating a recurrent neural network to finite-time convergence for solving time-varying Sylvester equation by using a sign-bi-power activation function," *Neural Process. Lett.*, vol. 37, no. 2, pp. 189–205, 2013.

[24] L. Xiao, J. Dai, R. Lu, S. Li, J. Li, and S. Wang, "Design and Comprehensive Analysis of a Noise-Tolerant ZNN Model With Limited-Time Convergence for Time-Dependent Nonlinear Minimization," *IEEE Trans. Neural Networks, Learn. Syst.*, vol. 31, no. 12, pp. 5339–5348, 2020.

[25] L. Xiao, Y. Zhang, Q. Zuo, J. Dai, J. Li, and W. Tang, "A Noise-Tolerant Zeroing Neural Network for Time-Dependent Complex Matrix Inversion Under Various Kinds of Noises," *IEEE Trans. Ind. Inf.*, vol. 16, no. 6, pp. 3757–3766, 2020. doi: 10.1109/TII.2019.2936877.

[26] J. Jin, and J. Gong, "A noise-tolerant fast convergence ZNN for Dynamic Matrix Inversion," *Int. J. Comput. Math.*, vol. 98, no. 11, pp. 2202–2219, 2021.

[27] L. Xiao, Z. Zhang, and S. Li, "Solving Time-Varying System of Nonlinear Equations by Finite-Time Recurrent Neural Networks, With Application to Motion Tracking of Robot Manipulators," *IEEE Trans. Syst. Man Cybern.: Syst.*, vol. 49, no. 11, pp. 2210–2220, 2019.

[28] J. Jin, L. Zhao, M. Li, F. Yu, and Z. Xi, "Improved zeroing Neural Networks, for finite time solving nonlinear equations," *Neural Comput. Appl.*, vol. 32, pp. 4151–4160, 2020.

[29] L. Jin, Y. Zhang, and S. Li, "Integration-enhanced Zhang neural network for real-time-varying matrix inversion in the presence of various kinds of noises," *IEEE Trans. Neural Networks, Learn. Syst.*, vol. 27, no. 12, pp. 2615–2627, 2016.

[30] L. Jin, Y. Zhang, S. Li, and Y. Zhang, "Noise-tolerant ZNN models for solving time-varying zero-finding problems: A control-theoretic approach," *IEEE Trans. Autom. Control*, vol. 62, no. 2, pp. 992–997, Feb. 2017.

[31] L. Xiao *et al.*, "A new noise-tolerant and predefined-time ZNN model for time-dependent matrix inversion," *Neural Networks*, vol. 117, pp. 124–134, 2019.

[32] C. Hu, J. Yu, Z. Chen, H. Jiang, and T. Huang, "Fixed-time stability of dynamical systems and fixed-time synchronization of coupled discontinuous Neural Networks," *Neural Networks*, vol. 89, pp. 74–83, 2017.

[33] C. Aouiti and F. Miaadi, "A new fixed-time stabilization approach for Neural Networks, with time-varying delays," *Neural Comput. Appl.*, vol. 32, pp. 3295–3309, 2020.

[34] A. Polyakov, "Nonlinear Feedback Design for Fixed-Time Stabilization of Linear Control Systems," *IEEE Trans. Autom. Control*, vol. 57, no. 8, pp. 2106–2110, 2012.

[35] J. Jin, J. Zhu, J. Gong, and W. Chen, "Novel activation functions-based ZNN models for fixed-time solving dynamic Sylvester equation," *Neural Comput. Appl.*, 2022, doi: 10.1007/s00521-022-06905-2.

[36] J. Jin and L. Qiu, "A robust fast convergence zeroing neural network and its applications to dynamic Sylvester equation solving and robot trajectory tracking," *J. Franklin Inst.*, vol. 359, pp. 3183–3209, 2022.

[37] J. Gong and J. Jin, "A better robustness and fast convergence zeroing neural network for solving dynamic nonlinear equations," *Neural Comput. Appl.*, 2021, doi: 10.1007/s00521-020-05617-9.

[38] F. Yu, H. Shen, Z. Zhang, Y. Huang, S. Cai, and S. Du, "A new multi-scroll Chua's circuit with composite hyperbolic tangent-cubic nonlinearity: Complex dynamics, Hardware implementation and Image encryption application," *Integration*, vol. 81, pp. 71–83, 2021.

[39] F. Yu *et al.*, "A 6D Fractional-Order Memristive Hopfield Neural Network and its Application in Image Encryption," *Front. Phys.*, vol. 10, p. 847385, 2022.

[40] D. Pazderski, "Application of transverse functions to control differentially driven wheeled robots using velocity fields," *Bull. Pol. Acad. Sci. Tech. Sci.*, vol. 64, no. 4, pp. 831–851, 2016. doi: 10.1515/bpasts-2016-0092.

[41] Z. Hendzel, "Collision free path planning and control of wheeled mobile robot using Kohonen self-organising map," *Bull. Pol. Acad. Sci. Tech. Sci.*, vol. 53, no. 1, pp. 39–47, 2005.

[42] W. Kowalczyk and K. Kozłowski, "Trajectory tracking and collision avoidance for the formation of two-wheeled mobile robots," *Bull. Pol. Acad. Sci. Tech. Sci.*, vol. 67, no. 5, pp. 915–924, 2019. doi: 10.24425/bpas.2019.128652.

[43] X. Ji, Q. Zhu, J. Wang, C. Cai, and J. Ma, "Mobile robot visual homing by vector pre-assigned mechanism," *Bull. Pol. Acad. Sci. Tech. Sci.*, vol. 67, no. 2, pp. 213–227, 2019.

[44] J. Jin, "A robust zeroing neural network for solving dynamic nonlinear equations and its application to kinematic control of mobile manipulator," *Complex Intell. Syst.*, vol. 7, pp. 87–99, 2021.

[45] J. Jin and J. Gong, "An interference-tolerant fast convergence zeroing neural network for Dynamic Matrix Inversion and its application to mobile manipulator path tracking," *Alexandria Eng. J.*, vol. 60, pp. 659–669, 2021.

[46] L. Xiao and Y. Zhang, "A New Performance Index for the Repetitive Motion of Mobile Manipulators," *IEEE Trans. Cybern.*, vol. 44, no. 2, pp. 280–292, 2014.

[47] D. Chen, S. Li, F.J. Lin, and Q. Wu, "New Super-Twisting Zeroing Neural-Dynamics Model for Tracking Control of Parallel Robots: A Finite-Time and Robust Solution," *IEEE Trans. Cybern.*, vol. 50, no. 6, pp. 2651–2660, 2020.